

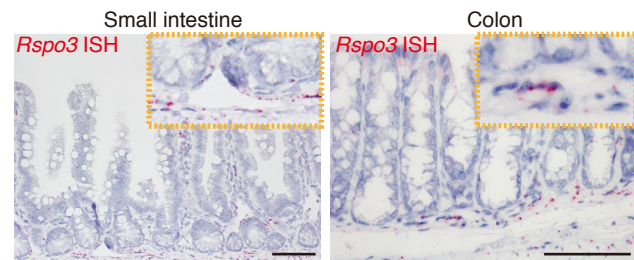
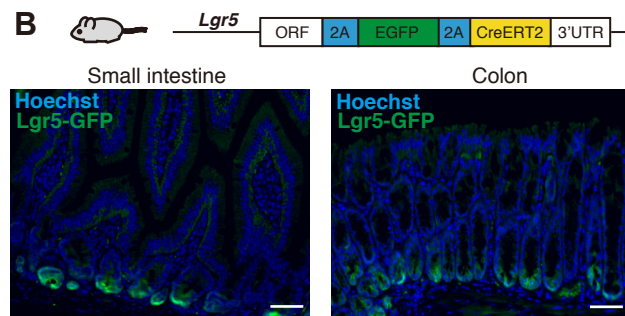
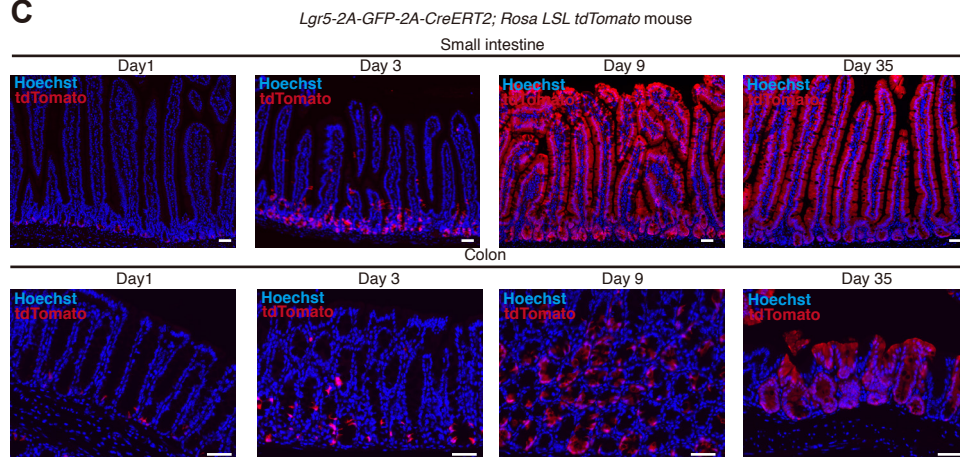
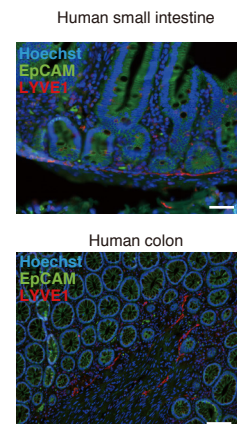
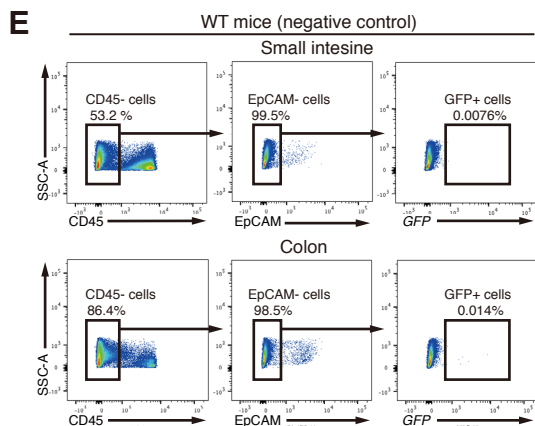
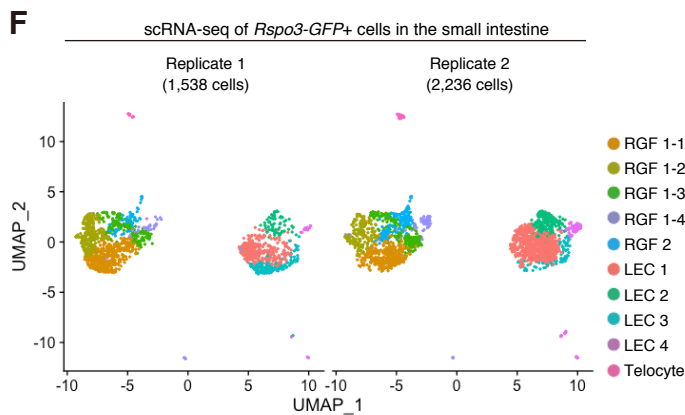
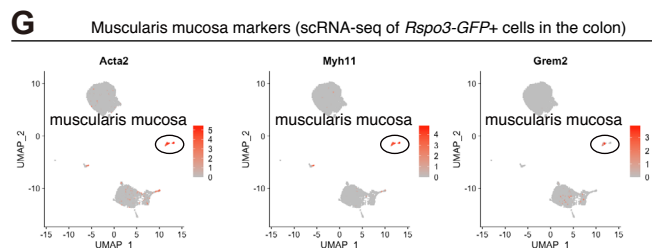
Figure S1**A****B****C****D****E****F****G**

Figure S1. RSPO3+ LECs reside near Lgr5+ ISCs, Related to Figure 1 and Figure 2

(A) *Rspo3* mRNA expression in the small intestine and colon by ISH.

(B) Schematic (top) of new *Lgr5-2A-GFP-2A-CreERT2* mice. Immunofluorescence (IF) shows that *Lgr5-GFP* is expressed in nearly all the crypts of both the small intestine and colon. The image represents one of 6 biological replicates.

(C) Lineage tracing using *Lgr5-2A-GFP-2A-CreERT2; Rosa-LSL-tdTomato* mice reveals that *Lgr5-GFP*⁺ cells self-renew for the long-term and give rise to differentiated progeny cells of the small intestine and colon. The image represents one of 3 biological replicates.

(D) IF for LYVE1 and EpCAM in the human small intestine and colon. Related to Figure 1D.

(E) Control (mouse without *Rspo3-GFP*) FACS plot to show that GFP⁺ cells of the *Rspo3-GFP* mice in Figure 1E are not detected in control mice. Related to Figure 1E.

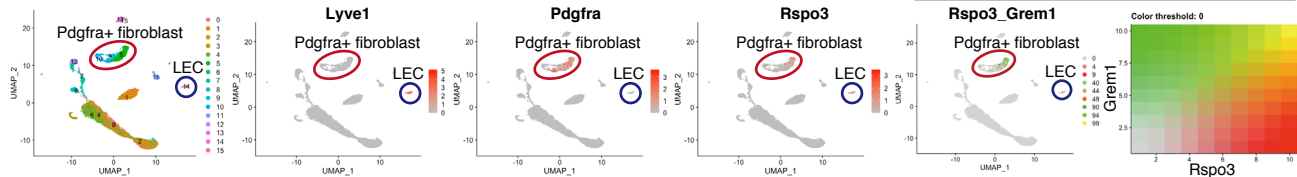
(F) Individual UMAP plots for each replicate of scRNA-seq of the small intestinal *Rspo3-GFP*⁺ stromal cells demonstrate the consistent clustering patterns among the replicates. Related to Figure 2A.

(G) Relative expression of *Acta2*, *Myh11*, and *Grem2* (muscularis mucosa cell marker genes), and *Pdgfra* (negative marker for muscularis mucosa cells) onto the UMAP plot of scRNA-seq of colonic *Rspo3-GFP*⁺ cells. Related to Figure 2E.

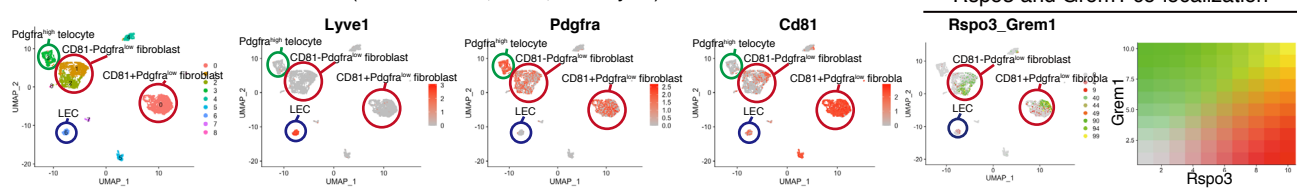
Scale bar, 50 μ m (A, B, C, D).

Figure S2

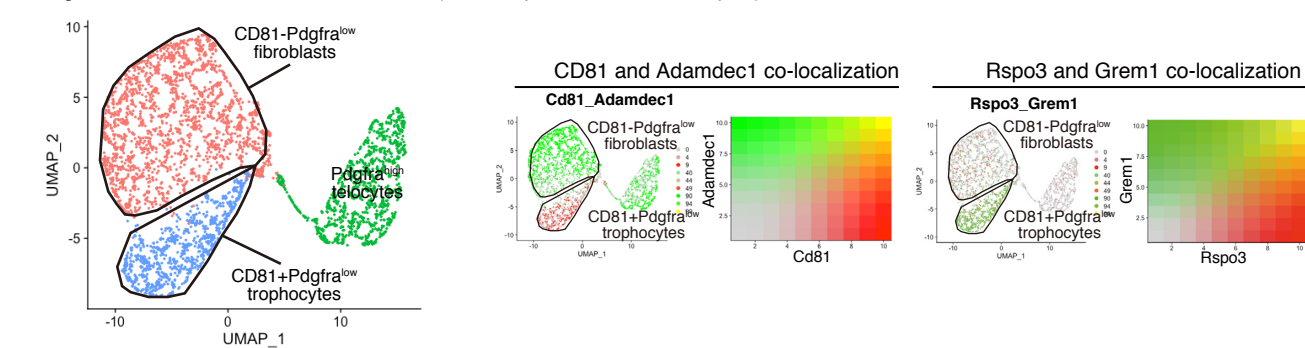
A Stromal cells in the mouse small intestine (McCarthy et al., 2020, reanalysis)



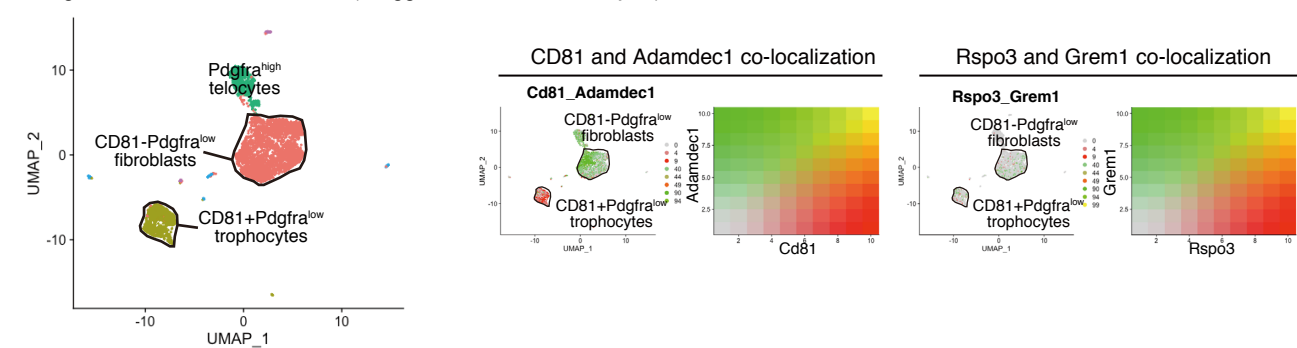
B Stromal cells in the mouse colon (Kinchen et al., 2018, reanalysis)



C Pdgfra⁺ cells in the mouse small intestine (McCarthy et al., 2020, reanalysis)



D Pdgfra⁺ cells in the mouse colon (Brugger et al., 2020, reanalysis)



E Stromal cells in the human colon (Kinchen et al., 2018, reanalysis)

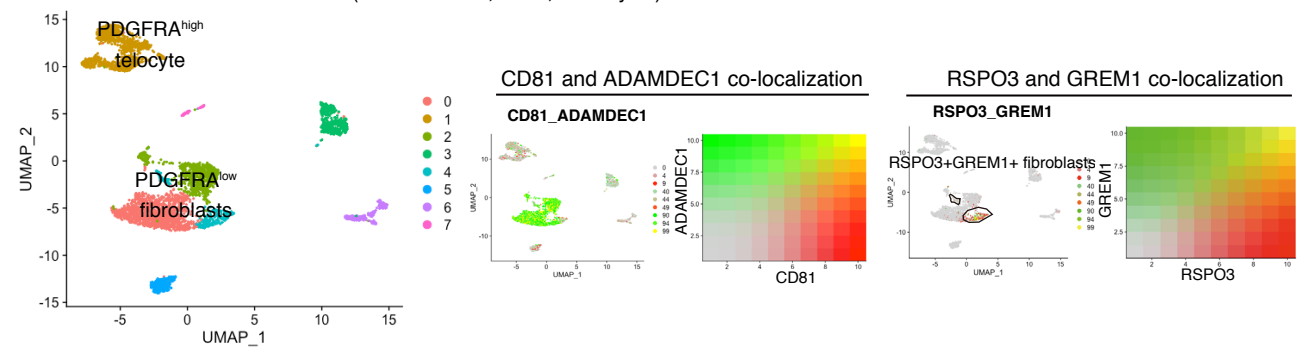


Figure S2. RSPO3 expression in the small intestinal and colonic stromal cells (reanalysis of public datasets). Related to Figure 1 and Figure 2

(A) Uniform manifold approximation and projection (UMAP) of scRNA-seq of small intestinal stromal cells (McCarthy et al., 2020, reanalysis). *Rspo3* is expressed by *Lyve1*⁺ LEC cluster and by a subset of *Pdgfra*⁺ fibroblast cluster. *Rspo3*⁺ cells in the *Pdgfra*⁺ fibroblasts cluster co-express *Grem1*.

(B) UMAP of scRNA-seq of colonic stromal cells (Kinchen et al., 2018, reanalysis). *Rspo3* is expressed by *Lyve1*⁺ LEC cluster and by a subset of *Pdgfra*^{low} fibroblasts (both *Cd81*-*Pdgfra*^{low} fibroblasts and *Cd81*+*Pdgfra*^{low} fibroblasts). A subset of *Rspo3*⁺ cells in the *Pdgfra*^{low} fibroblast clusters co-express *Grem1*.

(C) UMAP of scRNA-seq of small intestinal *Pdgfra*⁺ cells (McCarthy et al., 2020, reanalysis). The expressions of *Cd81* and *Adamdec1* are mutually exclusive. *Rspo3*⁺ cells are detected both in the *Cd81*⁺*Adamdec1*⁻*Pdgfra*^{low} trophocyte and *Cd81*⁻*Adamdec1*⁺*Pdgfra*^{low} fibroblast clusters, and these *Rspo3*⁺ cells frequently co-express *Grem1*.

(D) UMAP of scRNA-seq of colonic *Pdgfra*⁺ cells (Brugger et al., 2020, reanalysis). The expressions of *Cd81* and *Adamdec1* are mutually exclusive. *Rspo3*⁺ cells are detected both in the *Cd81*⁺*Adamdec1*⁻*Pdgfra*^{low} trophocyte and *Cd81*⁻*Adamdec1*⁺*Pdgfra*^{low} fibroblast clusters, and these *Rspo3*⁺ cells frequently co-express *Grem1*.

(E) UMAP of scRNA-seq of human colonic stromal cells (Kinchen et al., 2018, reanalysis). The expressions of *CD81* and *ADAMDEC1* are ubiquitous in *PDGFRA*^{low} fibroblasts and not mutually exclusive. *RSPO3*⁺*GREM1*⁺ cells are detected in a subset of *PDGFRA*^{low} fibroblasts.

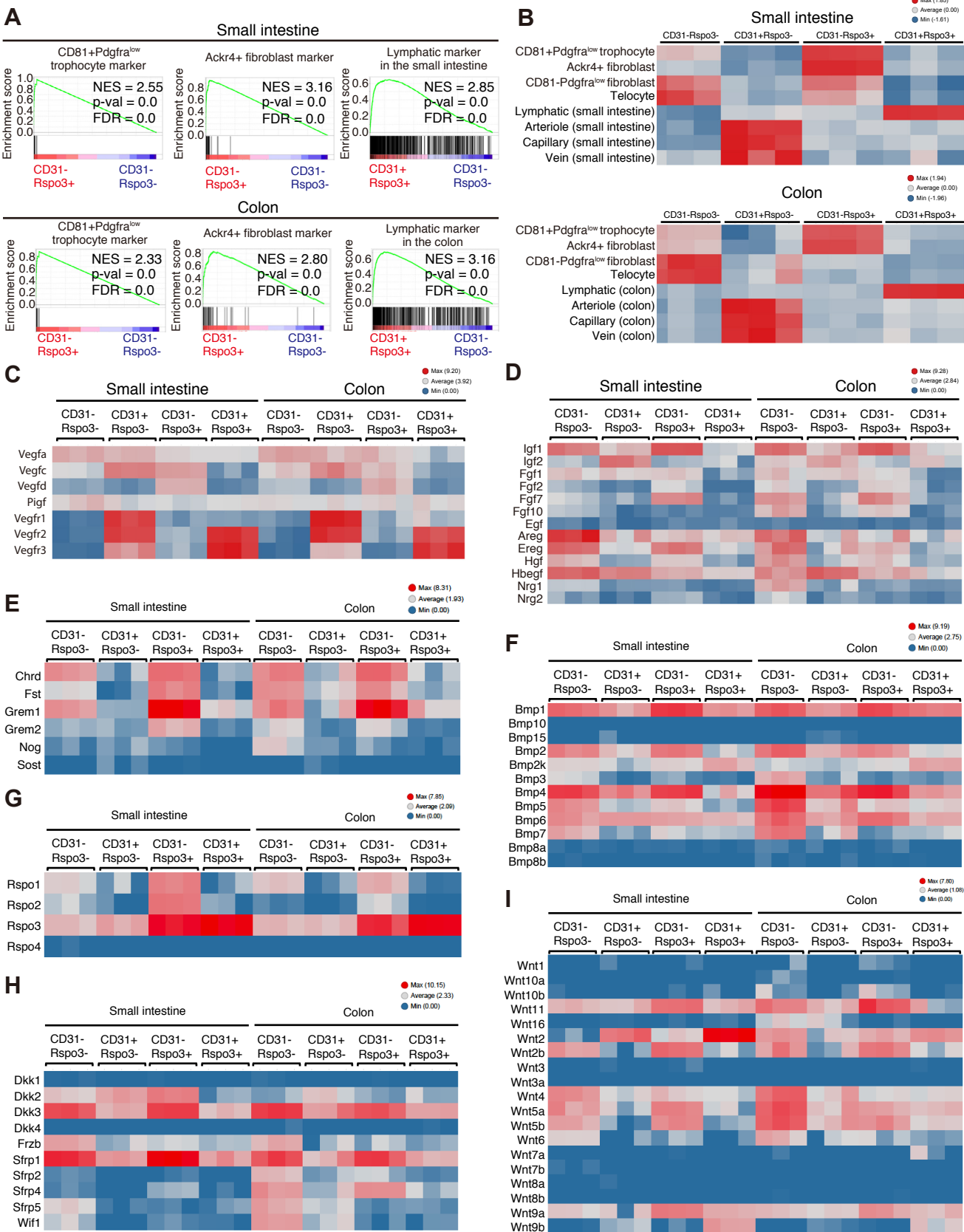
Figure S3

Figure S3. RNA-seq on CD31-Rspo3-GFP-, CD31+Rspo3-GFP-, CD31-Rspo3-GFP+, and CD31+Rspo3-GFP+ cells, Related to Figure 3

(A) GSEA of CD81+Pdgfra^{low} trophocyte markers, Ackr4+ fibroblast markers, and lymphatic markers. FDR, false-discovery rate; NES, normalized enrichment score.

(B) The heatmap of single sample GSEA (ssGSEA).

(C-I) The heatmap of gene expressions for angiogenic factors (C), growth factors (D), BMPi (E), BMP (F), RSPO (G), WNT antagonist (H), and WNT (I) using RNA-seq on CD31-*Rspo3-GFP*-, CD31+*Rspo3-GFP*-, CD31-*Rspo3-GFP*+, and CD31+*Rspo3-GFP*+ cells from the small intestine and colon.

n = 3 mice per group.

Figure S4

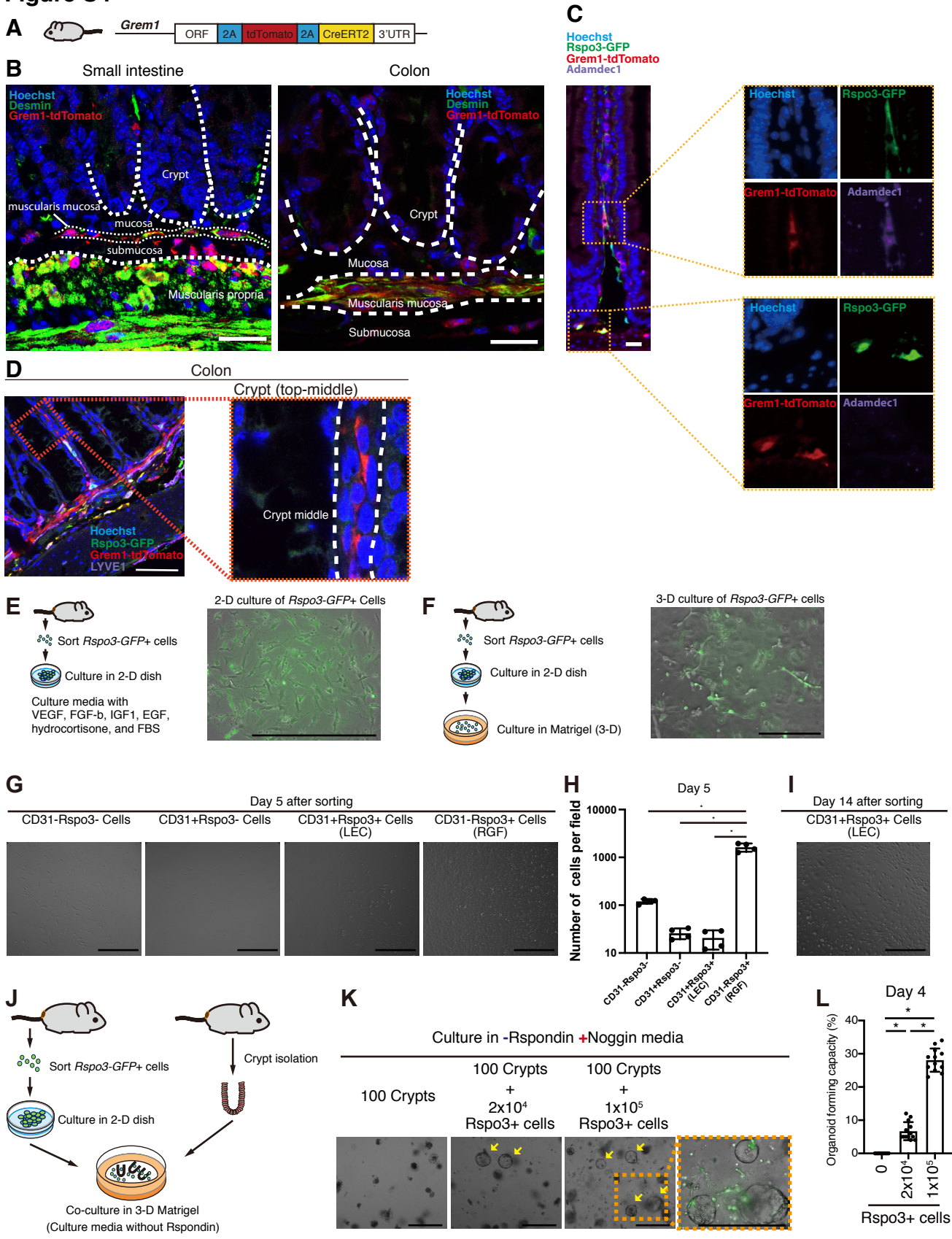


Figure S4. Expression pattern of GREM1 and RSPO3 and establishment of RSPO3+ stromal cell culture, Related to Figure 3 and Figure 4

(A) Schematic of *Grem1-tdTomato-CreERT2* mouse.

(B) Confocal microscopy of immunofluorescence (IF) for *Grem1-tdTomato* and Desmin, showing that *Grem1-tdTomato* is expressed by a subset of lamina propria and submucosal stromal cells, but is also strongly expressed by Desmin+ muscularis propria and muscularis mucosa cells.

(C) IF for *Rspo3-GFP*, *Grem1-tdTomato*, and Adamdec1 reveals that RGFs that are close to the crypt bottoms do not express Adamdec1 whereas RGFs infrequently detected in the villus core next to lacteals co-express Adamdec1.

(D) GREM1+RSPO3- cells at the middle-top zone of colonic crypts. lower magnification image is adapted from Figure 3E.

(E-F) 2-D (E) and 3-D (F) culture of sorted *Rspo3-GFP+* stromal cells from the small intestine.

(G-H) Images (G) and quantification (H) of 2-D culture of sorted CD31⁻*Rspo3-GFP*⁺, CD31⁺*Rspo3-GFP*⁺, CD31⁺*Rspo3-GFP*⁻, and CD31⁻*Rspo3-GFP*⁻ cells from the small intestine at day 5.

(I) Image of 2-D culture of CD31⁺*Rspo3-GFP*⁺ cells (LECs) from the small intestine at day 14 shows the stable expansion of LECs.

(J) Schematic of heterotypic co-culture of RSPO3+ stromal cells and the intestinal epithelial crypts.

(K-L) Representative images (K) and quantification (L) of co-culture of small intestinal RSPO3+ stromal cells (0, 2x10⁴, 1x10⁵) and the crypts in the culture media supplemented with Noggin, but not with RSPO. n = 12 - 13 from 3 mice per group. Arrows indicate organoid formation.

One-way analysis of variance (ANOVA) with post-hoc Tukey's multiple comparison (H, L). Data are mean ± SD.

*p < 0.05. Scale bar, 20 μm (B, C, E, F, G, I, K), 50 μm (D).

Figure S5. Niche RSPO3 loss reduces WNT signaling and proliferation in the crypt, Related to Figure 5.

(A-G) Comprehensive histochemical and immunohistochemical/fluorescence analyses in the small intestine and colon after inducing RSPO3 loss in LECs, RGFs, or both. Immunohistochemistry for Ki67 (A) and Lysozyme (B); PAS staining (C); ISH for *Rspo3* (D), *Axin2* (E), and *Ascl2* (F). Quantification of Ki67+ cells (per crypt), Lysozyme+ cells (per crypt), and goblet cells (percentage in the epithelial cells) (G) (n = 50 from 6 mice per group).

(H) Porcupine inhibitor LGK974 was administered (daily oral gavage, 5 mg/kg) to the mice after RSPO3 deletion. Whereas control mice or the mice with partial RSPO3 stromal loss (i.e., *Grem1-CreERT2; Rspo3 f/f* mice or *Prox1-CreERT2; Rspo3 f/f* mice) did not show any architectural changes, mice with complete RSPO3 stromal loss (i.e., *Grem1-CreERT2; Prox1-CreERT2; Rspo3 f/f* mice) illustrated significant crypt degeneration/drop-out in the intestines on day 8 of treatment. The image represents one of 4 biological replicates per group.

One-way analysis of variance (ANOVA) with post-hoc Tukey's multiple comparison (G). For box-and-whisker plots (G), data were expressed as box-and-whisker from the minimum to the maximum. *p < 0.05. N.S. not significant.

Scale bar, 20 μ m (A, B, C, D, E, F, H).

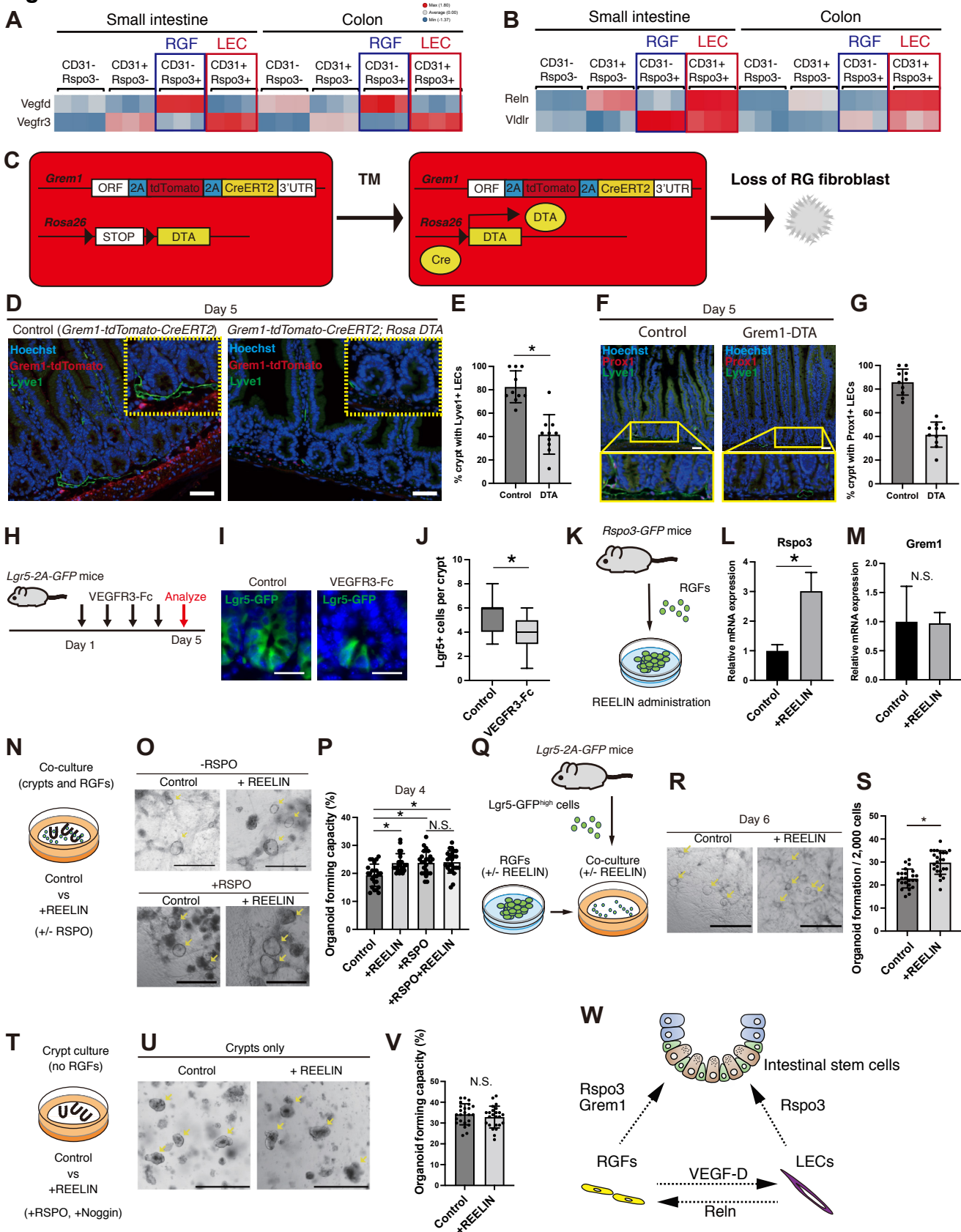
Figure S6

Figure S6. Cross-regulation between RGFs and LECs, Related to Figure 5

(A-B) Heatmap of RNA-seq on CD31-*Rspo3*-GFP-, CD31+*Rspo3*-GFP-, CD31-*Rspo3*-GFP+, and CD31+*Rspo3*-GFP+ cells in the small intestine and colon. RGFs express *Vegfd*; LECs express its receptor (*Vegfr3*) (A). LECs express *Reln*; RGFs express its receptor (*Vldlr*) (B). n = 3 mice per group.

(C) Schematic for RG fibroblast ablation experiment.

(D-G) Immunofluorescence for *Grem1*-tdTomato and LYVE1 (D), Prox1 and LYVE1 (F) and the percentage of crypts with LYVE+ LECs (E) or Prox1+ LECs (G) in *Grem1*-tdTomato-*CreERT2* (control) and *Grem1*-tdTomato-*CreERT2*; *Rosa DTA* mice. n = 10.

(H) Schematic for soluble VEGFR3 receptor administration experiment.

(I-J) Representative images (I) and quantification (J) of *Lgr5*-GFP+ cells after soluble VEGFR3 receptor administration. n = 50 crypts from 4 mice per group.

(K) Schematic for the treatment of RGF culture with REELIN.

(L-M) qRT-PCR of *Rspo3* and *Grem1* in RGFs after REELIN treatment. n = 6 and n = 3, respectively.

(N) Schematic of REELIN treatment to the co-culture of crypts and RGFs in media with/without RSPO.

(O-P) Representative images (O) and quantification of organoid forming capacity (P) in the co-culture of crypts and RGFs in media with/without REELIN and with/without RSPO. n = 24 from 3 mice per group.

(Q) Schematic of co-culture experiments of sorted *Lgr5*-GFP^{high} ISCs and REELIN-pretreated RGFs.

(R-S) *Lgr5*-GFP^{high} ISC-derived organoid formation is modestly elevated when RGFs were pretreated with REELIN. Representative images (R) and quantification (S). n = 24 from 3 mice per group.

(T) Schematic of REELIN treatment to crypt culture.

(U-V) Representative images (U) and quantification of organoid forming capacity (V) in the crypt culture with Noggin and RSPO supplementation with or without REELIN administration. n = 24 from 3 mice per group.

(W) Schematic of proposed cross-regulation between RGFs and LECs.

Unpaired two-tailed t-tests (E, G, J, L, M, S, V). One-way ANOVA (P). Data are mean \pm SD (E, G, P, S, V) and mean \pm SEM (L, M). For box-and-whisker plots (J), data were expressed as box-and-whisker from the minimum to the maximum. *p < 0.05. N.S. not significant. Scale bar, 50 μ m (D, F, I), 20 μ m (O, R, U).

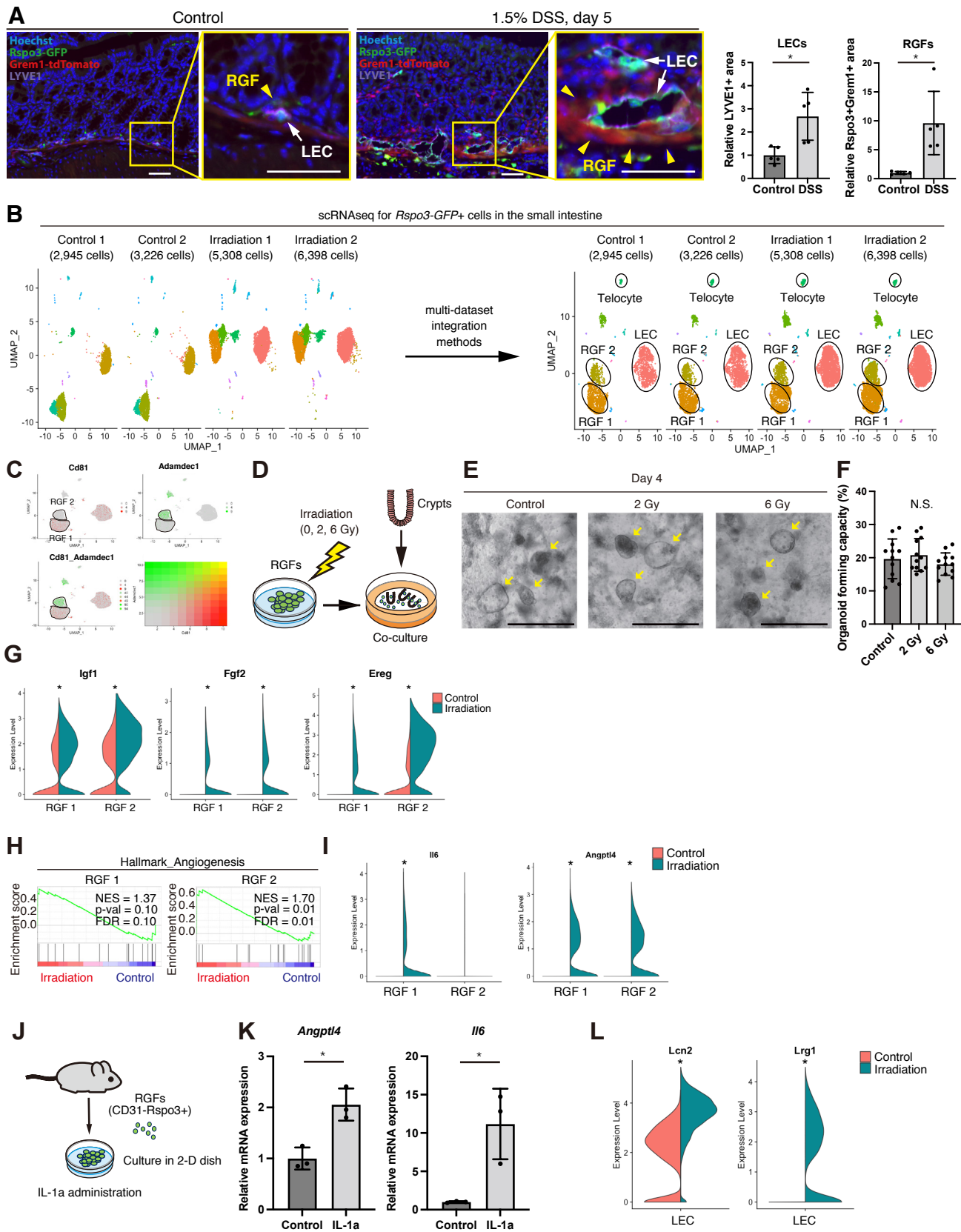
Figure S7

Figure S7. Roles of LECs and RGFs in normal homeostasis and regeneration after injury, Related to Figure 6 and Figure 7

(A) Immunofluorescence for *Rspo3-GFP*, *Grem1-tdTomato*, and LYVE1 in the DSS-induced colitis model at day 6 of 1.5% DSS administration. Yellow arrowheads indicate RGFs. White arrows indicate LECs. LYVE1+ areas (LECs) and *Rspo3-GFP+Grem1-tdTomato+* areas (RGFs) were quantified. (n = 5 fields from 3 mice per group)

(B) Individual UMAP plots of scRNA-seq of small intestinal *Rspo3-GFP+* cells 3 days post-irradiation before (left) and after (right) applying multi-dataset integration methods (Control, n = 2 mice (2,945 cells and 3,226 cells); irradiation, n = 2 mice (5,308 cells and 6,398 cells)).

(C) Relative expression of *Cd81* and *Adamdec1* onto the UMAP plot of *Rspo3-GFP+* cells from both control and irradiation mice. n = 17,877 cells from 4 mice.

(D) Schematic of co-culture experiments post-irradiation.

(E-F) Representative images (E) and quantification of organoids (F) at day 4 of co-culture of irradiated RGFs and crypts. n = 12 from 3 mice per group.

(G) Violin plots for *Igf1*, *Fgf2*, and *Ereg* expressions.

(H) GSEA of HALLMARK Angiogenesis genes in irradiation vs control mice from RGF 1 cluster (left) and RGF 2 cluster (right) of scRNA-seq.

(I) Violin plots for *Il6* and *Angptl4* expressions.

(J) Schematic for the treatment of RGF culture with IL-1a. Adapted from Figure 7I.

(K) qRT-PCR of *Il6* and *Angptl4* mRNA expressions from RGFs 24 hours after IL-1a treatment. n = 3 mice per group.

(L) Violin plots for *Lcn2* and *Lrg1* expressions comparing control and irradiation mice in LEC cluster of scRNA-seq. One-way analysis of variance (ANOVA) with post-hoc Tukey's multiple comparison (F). Unpaired two-tailed t-tests (A, K). Wilcox test (G, I, L). Data are mean \pm SD. *p < 0.05. N.S. not significant. Scale bar, 50 μ m (A), 20 μ m (E).